Am J Nucl Med Mol Imaging 2019;9(2):110-126
www.ajnmmi.us /ISSN:2160-8407/ajnmmi0093583

Review Article

Update on imaging-based diagnosis of acute renal allograft rejection

Richard Köhnke[1], Dominik Kentrup[1,2], Katharina Schütte-Nütgen[1], Michael Schäfers[3,4], Uta Schnöckel[3], Verena Hoerr[5,6], Stefan Reuter[1]

[1]Department of Medicine, Division of General Internal Medicine, Nephrology and Rheumatology, University Hospital of Muenster, 48149 Muenster, Germany; [2]Department of Medicine, Division of Nephrology, The University of Alabama at Birmingham (UAB), 35294 Birmingham Alabama, US; [3]Department of Nuclear Medicine, University Hospital of Muenster, 48149 Muenster, Germany; [4]European Institute for Molecular Imaging, University of Muenster, 48140 Muenster, Germany; [5]Department of Clinical Radiology, University Hospital of Muenster, 48149 Muenster, Germany; [6]Institute of Medical Microbiology, Jena University Hospital, Am Klinikum 1, 07747 Jena, Germany

Received March 9, 2019; Accepted April 12, 2019; Epub April 15, 2019; Published April 30, 2019

Abstract: Kidney transplantation is the preferred treatment for patients with end-stage renal disease. Despite effective immunosuppressants, acute allograft rejections pose a major threat to graft survival. In early stages, acute rejections are still potentially reversible, and early detection is crucial to initiate the necessary treatment options and to prevent further graft dysfunction or even loss of the complete graft. Currently, invasive core needle biopsy is the reference standard to diagnose acute rejection. However, biopsies carry the risk of graft injuries and cannot be immediately performed on patients receiving anticoagulation drugs. Therefore, non-invasive assessment of the whole organ for specific and rapid detection of acute allograft rejection is desirable. We herein provide a review summarizing current imaging-based approaches for non-invasive diagnosis of acute renal allograft rejection.

Keywords: Acute allograft rejection, imaging, noninvasive, ultrasound, PET, SPECT, MRI, kidney transplantation

Introduction

Kidney transplantation (KTx) is the treatment of choice for patients with end-stage renal disease [1, 2]. Despite modern immunosuppressive regimens offering good patient and graft survival rates, acute rejection (AR) in form of acute cellular as well as acute antibody-mediated rejection (AMR) remains a problem after KTx by still decreasing patient and graft survival rates on occurrence [3, 4].

To limit the damage resulting from AR, early detection and treatment of AR is essential. At present, renal allograft biopsy remains the "gold-standard" for diagnosis of AR. Although an ultrasound-guided core needle biopsy of renal allografts (with indication) is relatively safe, due to its invasive nature, a biopsy potentially bears complications for the patient as the procedure itself may cause graft bleeding or result in the development of arteriovenous fistulae. Further, an interobserver variability and sampling errors limit its benefit [5, 6]. Therefore, a non-invasive assessment to detect AR is desired. Urinary and plasma biomarkers of acute and chronic renal AR have been extensively studied. Many studies either lack the essential controls or were unable to demonstrate sufficient sensitivity or specificity of the marker, when compared to crucial differential diagnoses such as acute tubular necrosis (ATN) or calcineurin-inhibitor toxicity.

Medical imaging techniques have significantly improved during the last years offering a high level of temporal and spatial resolution by now. They are commonly available and are, therefore, extensively included in patients' clinical management. We herein review current imaging-based state of the art approaches for non-invasive diagnostics of acute renal transplant rejection. A summarizing overview is provided in **Table 1**.

Table 1. Comprehensive Overview of imaging methods

Modality		Imaging agent	Advantages	Disadvantages	Ref.
Ultrasound		Optional	Rapid, bed side, non-invasive, no radiation, commonly available, low costs	Operator dependent	
(Color) Doppler	i.e. RI	None		Influence of extra renal factors [5, 8, 9], low sensitivity, low specificity [12]	[5, 7-10, 12]
	SDI	None			[7]
Power Doppler		None	Analysis of intensity of the signal (in contrast to color doppler: analysis of the flow)	Low specificity	[13]
Elastography		None		Low specificity	[14]
	SWEI				[14]
AFRI		None		Low specificity	[15, 16]
	VISR	None		AR was not addressed in study [17]	[17]
CEUS		Microbubble-based agents	Safe, simple. Relatively high sensitivity and specificity [18]	Potentially immunogenic antibodies	[18]
		Targeted microbubbles (i.e. T-lymphocytes) [19]		Preclinical method, antibody-mediated AR not addressed	[19, 20]
		Targeted microbubbles (i.e. C4d) [21]		Preclinical method, limitation in cases of C4d-negative AMR	[21]
MRI					
DWI MRI		None	No contrast agents (gadolinium) needed [25]	DWI alone not suitable to differentiate the underlying causes of acute allograft dysfunction	[25, 26]
	ADC			Calculated parameter; low specificity [5]	
	DTI		Good correlation with renal function [30]		[28, 30]
	ASL			Still under development [5]	[5, 41, 42]
BOLD MR		Deoxygenated hemoglobin (endogenous agent) [5]	May be useful to differentiate AR from ATN [33]	Endogenous contrast agent	[5, 31, 33]
(USPIO)-enhanced dynamic MRI		Ultrasmall supermagnetic iron oxide particle-loaded macrophages (i.e.) [44, 45]			[5, 44, 45]
		Iron oxide particles to label T-cells [46]		Rat model. Difficult to distinguish between live and dead labeled cells [47]	[46, 47]
CEST	GlucoCEST [48, 49]	Naturally occurring D-glucose [49]	High sensitivity, Detection of treatment response [49]	Rat model	[48, 49]
Contrast Enhanced MRI	DCE, MRNU	Gadolinium-based contrast agents [34]	No radiation	Risk of gadolinium contrast-induced nephrogenic systemic fibrosis [38]	[5, 34, 35, 38]
Computed Tomography					
Perfusion CT		IV-(radio-) contrast agents (i.e. iodinated agents)		Radiation, side effects of IV-contrast-agents	[5]
Conventional nuclear imaging					
SPECT		Isotopes are (i.e.) ^{111}In, ^{67}Ga, ^{123}I and ^{99m}Tc [53]	Operator indepency, Availability of non-nephrotoxic tracers [5]		[5, 29, 53]
		Radiolabed white blood cells [55], labled mononuclear cells [60]	Possible detection of rejection and discrimination from ATN [60]	Immunogenicity-related side-effects (allergic reactions)	[5, 55, 60]

		Labled antibodies (i.e. CD3) [62]		Methods are limited to detect the intra- or peri-vascular antigens [5, 65]	[5, 60, 62, 65]
		Radiolabeled ligands [66]			[66]
		Reporter gene-mediated methods, radiolabeled regulatory T cells [67]			[67]
		^{99m}Tc-recombinant complement receptor 2 [68]		Clinical studies are missing	[68]
		DTPA, MAG3 [69, 70, 73, 74]	Detection of AR and discrimination from ATN	Specificity for AR is low	[69, 70, 73, 74]
Positron emission tomography					
	PET-CT	^{18}F-Fluordeoxyglucose [78]	Detection of AR [79], possible discrimination from ATN [81]	Rat model	[78-81]
		^{18}F-FDG labelled T-cells [81]	Positive correlation between the tracer-uptake in the allograft and the histologic degree of rejection [79], possible monitoring of treatment efficacy [79, 83], 100% sensitivity [5]	Production of labled T-cells is time consuming [5], low specificity	[5, 79, 81, 83]

AR, acute rejection; ADC, apparent diffusion coefficient; AFRI, acoustic radiation force impulse imaging; AMR, acute antibody-mediated rejection; ASL, arterial spin labeling; ATN, acute tubular necrosis; BOLD, blood-oxygen level-dependent; CT, computed tomography; CEST, chemical exchange saturation transfer; CEUS, contrast-enhanced ultrasound; DCE, dynamic contrast enhanced; DTI, diffusion tensor imaging; DTPA, ^{99m}Tc-diethylenetriaminepentaacetic acid; DWI, diffusion-weighted imaging; FDG, F-Fluordeoxyglucose; MAG3, ^{99m}Tc-mercaptoacetyltriglycine; MR, magnetic resonance; MRI, magnetic resonance imaging; MRNU, MR nephro-urography; PET, positron emission tomography; PI, pulsatility index; RI, resistive index; SDI, serial duplex index; SPECT, single photon emission computed tomography; SWEI, shear-wave-sonoelastography; USPIO, ultrasmall supermagnetic iron oxide.

Ultrasound

Ultrasonography of renal allografts is a clinical standard method applied to manage kidney transplanted patients. Ultrasound examination can be used to visualize the possible findings of AR, such as an enlargement of the transplant caused by the swelling and alteration of morphology, loss of corticomedullary differentiation, or changes in echogenicity. Furthermore, one can assess renal blood flow using the Doppler and Power ultrasound. The introduction of ultrasound contrast medium (to enhance echogenicity) in recent years has led to vast improvements in the technique and the development of contrast-enhanced ultrasound (CE-US). Further techniques such as ultrasound elastography have been evaluated in renal transplanted patients recently. Overall, ultrasonography offers several advantages including cost-effectiveness, bed side availability and real-time imaging, but has, at the same time (at least at present), limitations in sensitivity and specificity for the diagnosis of AR. Moreover, it has a certain interobserver variability and needs to be performed by experienced investigators. We will discuss several ultrasound applications proposed for the assessment of the renal allograft and AR.

To evaluate the function of the transplant and to detect acute transplant dysfunction, the assessment of the resistive index (RI), a non-invasive measure of vascular resistance and elastic compliance, was proposed [7]. Unfortunately, the intrarenal RI is affected by systemic parameters including vascular compliance, pulse pressure, heart rate, and rhythm (i.e. atrial fibrillation) [8]. To note, a recipient's age is the strongest determinant of high RIs because systemic arteriosclerosis is age-dependent [9]. Interestingly, an RI of above 0.8 is even associated with increased mortality [9, 10]. Besides cellular AR, antibody-mediated rejection and ATN are associated with a higher RI [9]. Therefore, it is not surprising that data regarding the impact of the RI on allograft outcomes is controversially discussed [9-11]. Sensitivity and specificity of the RI to detect AR is low due to the aforementioned limitations e.g., Perrella et al. found a low sensitivity of 43% and a specificity of 76% in their study [12]. As an attempt to overcome some of these limitations, Meier et al. recently proposed the calculation of the so-called serial duplex index (SDI) by combining the cortex-pelvis proportions (CPPs), the RI, and the pulsatility index (PI) within one formula: (RI ratio X PI ratio)/CPP ratio. By doing so, they showed that the SDI could be used to distinguish between the ATN and vascular and cellular AR. However, the SDI was not developed to replace histologic examination of the allograft but rather to support the indication of transplant biopsy [7].

Shebel et al. proposed the Power Doppler sonography for the detection of transplant rejection. In contrast to the Color Doppler sonography, which provides information on the flow and frequency, the Power Doppler analysis provides information about the intensity (of the ultrasound signal) in the region of interest such as the renal cortex. In their study, cortical hypoperfusion was found in 93% of cases with AR as a constant Doppler sign. The authors suggested using a certain scoring system to differentiate AR from other pathologies like ATN. However, other authors found controversial results [13].

Ultrasound elastography non-invasively assesses the tissue stiffness and its elastic properties in response to an impinged force [14]. The authors state that elastography can differentiate stable allograft from acute and chronic allograft dysfunction. Several variants of this technique have been developed but only a few have been applied in the setting of renal transplantation. Unfortunately, the approaches lack specificity for identification of the underlying diseases.

Acoustic Radiation Force Impulse Imaging (ARFI) examines the elasticity of the tissue and is utilized to identify AR. In patients undergoing AR, the ARFI-values were elevated by more than 15% compared to other pathologies like calcineurin inhibitor toxicity and ATN [15]. Other studies used the AFRI to assess kidney dysfunction, either in native kidneys or in renal transplants, but the small study performed by Stock et al. was the only one addressing AR [16].

Viscoelastic response ultrasound (VISR) was used in a pilot *in vivo* study by Hossain et al. in 2017. VISR is an ARFI-based method to measure the viscoelastic properties of a tissue (renal transplant). The authors of the study conclude that i.e. chronic allograft nephropathy can be differentiated from other renal patholo-

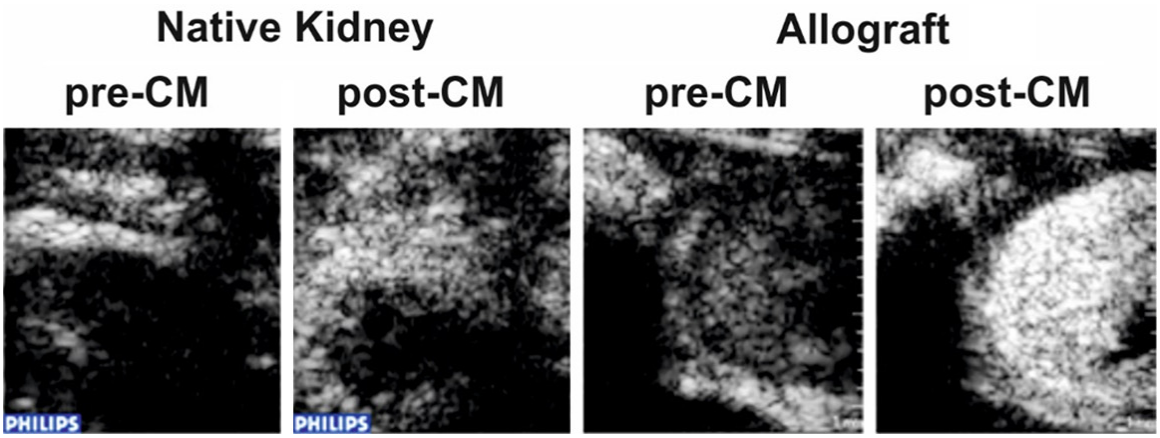

Figure 1. Representative ultrasound images of an allogeneically transplanted (aTX) rat kidney (graft) and its native control kidney (native) on day four post surgery (POD4). Depicted are examples of transversal images taken before (pre-CM) and 15 minutes after (post-CM) tail vein injection of anti-CD3-antibody labeled microbubbles. POD: post-operative day, CM: contrast media/microbubbles conjugated to anti-CD3 antibody.

gies like glomerulonephritis. This technique was proposed to improve the selectivity of biopsy candidates. AR was not addressed in this study [17].

To differentiate stable graft function from acute dysfunction - for instance like seen in AR-Ghonge et al. evaluated shear-wave-sonoelastography (SWEI). Interstitial fibrosis of the allograft increases the parenchymal stiffness values. In a group of 60 transplanted patients the authors were able to use parenchymal stiffness values to differentiate stable allograft function from acute dysfunction with 73.68% sensitivity and 80.65% specificity. The authors consider their method as an additional technique for the monitoring of KTx patients [14].

CEUS (contrast-enhanced ultrasound) is another promising technique recently described by others and us to assess AR. Basically an improvement on standard ultrasonography, CEUS' underlying principle is to greatly enhance the echogenicity of blood through the application of microbubble-based contrast agents. The application of these contrast agents is thought to be safe and simple. Some authors, like Mueller-Peltzer et al., demonstrated CEUS to have a sensitivity of 85.7% and a specificity of 100% in diagnosing AR in comparison to transplant biopsy [18]. CEUS can be not only used to assess common parameters, such as renal blood flow in real-time without affecting the renal (allograft) function, but can also be used for more advanced imaging methods [16]. As information of blood flow changes are rather unspecific, we developed CEUS for the detection of AR by using a microbubble-based contrast agent targeted specifically at the T-lymphocytes. During cellular AR, the T cells typically accumulate within the renal graft, causing inflammation, which can be visualized by using microbubbles specifically targeted at these cells by coupling the contrast agent to T cell-specific antibodies such as anti-CD3 (**Figure 1**). After application, this leads to an accumulation of the contrast agent within the renal graft, thus greatly improving the grafts echogenicity [19]. Using this approach, we could show that it can be applied to specifically detect AR-related T-lymphocytes even in the early stages of rejection; its signal intensity correlates with the severity of rejection. This promising preclinical method can also be used to differentiate AR from ATN and cyclosporine A (CSA) toxicity, as ATN and CSA did not lead to an increased signal [20]. However, acute antibody-mediated AR has not been investigated yet in this setting. This idea has been followed by Liao et al. who detected C4d deposition by CEUS in an *in vivo* rat renal transplantation model but might has a limitation in cases of C4d-negative AMR [21]. For illustration see **Figure 2**.

MRI

Different magnetic resonance imaging (MRI)-based approaches have been tested to non-invasively assess kidney allograft function. The MRI scanner detects signals from the hydrogen nuclei based on their magnetic behavior in re-

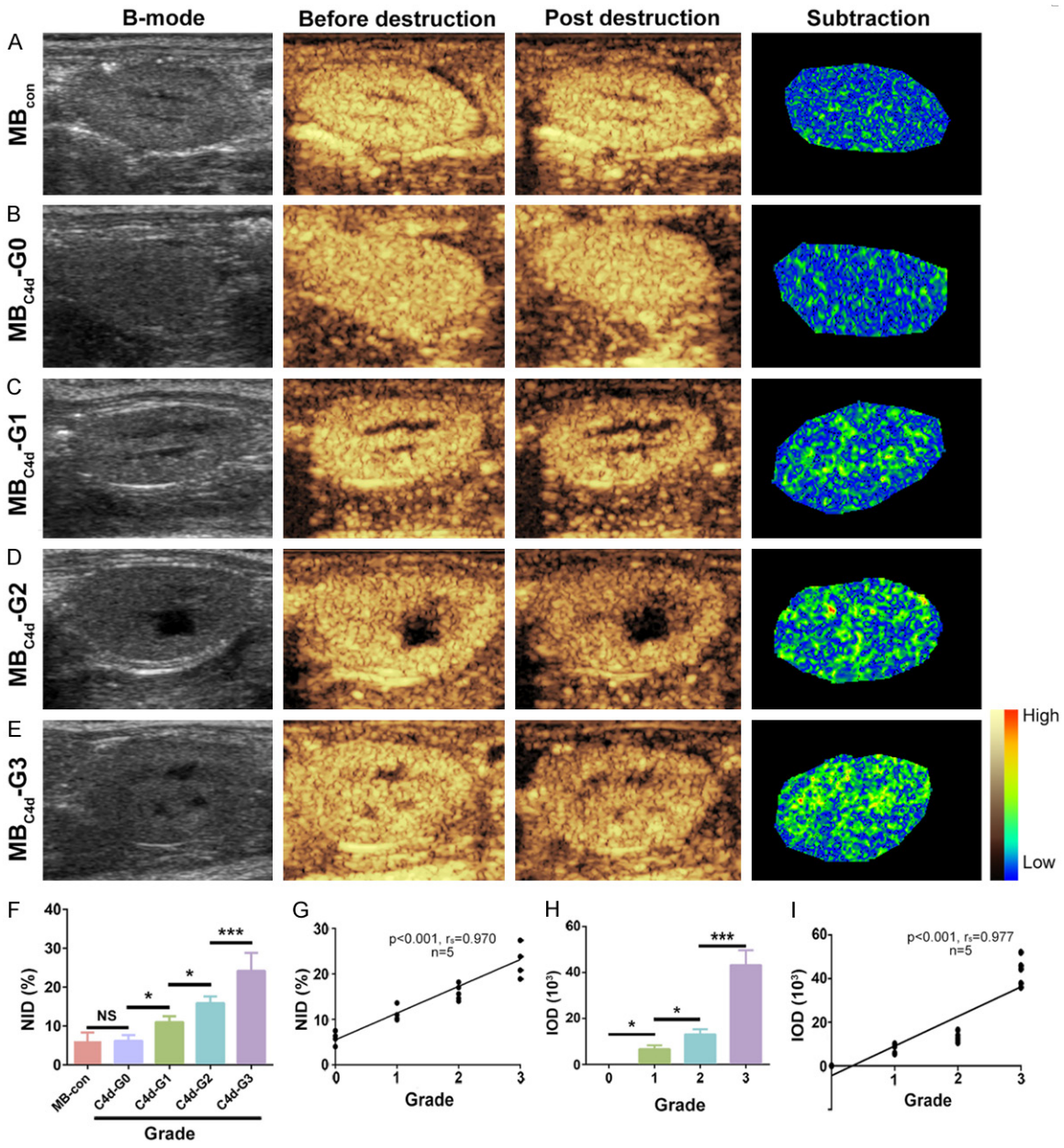

Figure 2. Qualitative and quantitative analysis of C4d deposition in the kidney. Control microbubbles (MBCon) and C4d targeted microbubbles (MBC4d) were injected into recipients and targeted ultrasound (US) imaging was obtained via a destructive-replenishment approach. To ensure the clearance of MBs in circulation, the interval between applications of MBCon and MBC4d was set to 30 min. A-E. Representative targeted US images of the MBcon group (n = 20), MBC4d-G0 group (SY grafts 3 d after transplantation; n = 5), MBC4d-G1 group (6 h after transplantation; n = 5), MBC4d-G2 group (1 d after transplantation; n = 5), and MBC4d-G3 group (3 d after transplantation; n = 5). F. The normalized intensity differences (NIDs) of different C4d grades (n = 20 in the MBcon group; n = 5 in each of other groups). G. Correlation analysis between NID and C4d grades (n = 5/group). H. The integrated optical density (IOD) of different C4d grades (n = 5/group). I. The correlation between IOD and C4d grades (n = 5/group). *P < 0.05; ***P < 0.001. This image has been taken with permission from the paper [21].

sponse to the radiofrequency impulses in a magnetic field. Thereby, different tissue characteristics, including intrinsic MR properties, such as the relaxation times T_1 and T_2, can be distinguished [22].

Although MRI is considered as a promising technique in nephrology, it has not yet been established in the routine follow-up of kidney transplanted patients [23]. There are functional and morphological MRI techniques: Morpho-

logical techniques search for changes in tissue contrast in the organ, such as the loss of the corticomedullary differentiation of the kidney. Huang et al. also showed that the comparison of T_1-values in the renal medulla and the renal cortex can be taken as a non-specific imaging marker of the declining organ function regardless of the underlying cause [24]. Functional MRI techniques measure (patho-) physiological changes in native or transplanted kidneys, such as perfusion, oxygenation, and inflammation [23].

Microstructure

By diffusion-weighted MRI (DWI MRI) the "Brownian" motion can be detected. The "Brownian" motion is the random movement of water molecules in tissues. It is influenced by tissue structures such as membranes and, thus, changes in the morphological tissue conditions. The role of DWI MRI for differentiation between AR and ATN was discussed recently [25]. According to Caroli et al. DWI MRI alone is not suitable to differentiate the underlying causes of acute allograft dysfunction from each other; a combination of different diffusion parameters such as apparent diffusion coefficient (ADC) or fractional anisotropy (FA) might overcome this limitation [26]. Using a mouse KTx model Hueper and colleagues showed that DWI and T_2-mapping can assess graft inflammation and edema formation in the course of i.e. rejection or ischemic renal injury [27].

By calculating the so called ADC the extent of diffusion of the water molecules can be quantified [28]. The ADC is influenced by the signal decay that is induced by the relative diffusion-based displacement of water molecules [29]. Thereby a decrease in ADC correlates with increased signal intensity on DWI. The ADC is affected by the tissue microstructure, which itself may be affected by conditions like ATN and other pathologies. In their review, Hanssen et al. summarized that the ADC is capable of detecting renal allograft dysfunction with high specificity, but has low specificity for the detection of AR. Other conditions may also influence (lower) this coefficient [5, 30]. In general, the diffusion motion is multi-directional and is called "isotropic diffusion" when influencing structures are absent. When diffusion motion is restricted to a direction, e.g., due to microstructures, it is called "anisotropic diffusion" [28]. To address the issue of anisotropic diffusion properties, a more sensitive form, termed diffusion tensor imaging (DTI), has been applied [30]. DTI allows the assessment of the fractional anisotropy (FA) of tissues, thereby considering the direction of diffusion [28]. There seems to be a good correlation of FA values of the renal medulla and the suspected allograft function. Interestingly, this correlation was absent for the cortex FA values [28].

Oxygenation

The distinction of AR and ATN conditions might also be possible via the so-called blood-oxygen level-dependent (BOLD) MR. Basically, this method uses deoxygenated hemoglobin as the endogenous contrast agent:

Levels of deoxyhemoglobin increase in tissues with lower oxygen concentration and shorten the transverse relaxation time constant T_2*. The apparent relaxation rate, R_2* (= $1/T_2$*), is - inversely - elevated [5]. BOLD MR can serve for the assessment of the renal parenchymal oxygenation concentration. In kidneys undergoing AR, a significantly lower medullary R_2*, corresponding to a higher oxygenation, was observed compared to kidneys with ATN [31, 32]. BOLD MRI might be helpful to differentiate AR from ATN [33].

Perfusion

Dynamic Contrast Enhanced MRI (DCE MRI) is a MRI method to assess vascular processes using gadolinium-based contrast agents [34]. The contrast agents are free filtered at the glomeruli but neither secreted nor reabsorbed in the tubules. Due to these characteristics, they facilitate the assessment of renal perfusion, glomerular filtration rate (GFR) and tubular function, all of which have been shown to be useful for the discrimination between AR and ATN [35]. Further, Kalb et al. described a patient who underwent MR Nephro-Urography (MRNU), a combination of functional and anatomical imaging, to detect antibody-mediated rejection; the results were supported by the clinical presentation and transplant biopsy. The authors suggested that the measurement of parenchymal signal changes and perfusion abnormalities can be used to identify patients with AR [35].

In contrast to kidneys with normal function, the cortical and medullary blood flow of grafts with AR is significantly altered. Particularly, the reduced medullary blood flow in grafts with AR seems to be typical [36]. An automated DCE MRI protocol for evaluation of renal allograft rejection was described by Khalifa et al. by safely separating grafts with AR from grafts without AR [37].

When applying contrast agent-based MRI, one has to pay attention to the rare side effect of gadolinium contrast-induced nephrogenic systemic fibrosis [38]. Gadolinium-based contrast agents can be categorized by their molecular structure and stability: ionic linear, nonionic linear, and macrocyclic chelates. Recent studies on the gadolinium deposits in the brain tissue questioned the safety of these contrast agents [39].

In 2/2018, the Drug commission of the German Medical Association informed all clinicians ("Rote-Hand Brief") that gadolinium accumulates in the brain, especially after the application of linear gadolinium-based contrast agents. Hence, they recommend the avoidance of intravenous application of such linear agents in other settings than in intra-articular imaging or liver MRI [40].

Arterial spin labeling (ASL) MRI is an approach for assessing organ function, especially for longitudinal perfusion studies. ASL MRI makes use of water protons of the arterial blood as the contrast agent [41]. Inflowing blood is selectively labeled by altering its longitudinal magnetization to have an opposite magnetization compared to the destination tissue. To determine tissue perfusion, the difference between a labeled image (tag) and a non-labeled image (control) can be used. ASL MRI has been successfully used to assess native and transplanted kidneys. For instance, Hueper et al. investigated kidney allografts in mice in the settings of acute and chronic rejection by ASL MRI. Impaired perfusion was linked to the extent of renal damage [41]. In humans, in congruence to these observations, one can find a significant lower cortical perfusion in renal grafts with an acute decrease in renal function compared to allografts with good long-term function and good function in the postoperative period [42].

Inflammation

Several studies have utilized nanoparticles to detect specific immune cells or immune proteins in the kidney to non-invasively detect inflammation (for review see [43]). In the context of renal transplantation, Hauger et al. and Chae et al. described the successful usage of supermagnetic iron oxide (SPIO) particle-loaded macrophages to differentiate between causes of allograft dysfunction [44, 45]. Ultrasmall supermagnetic iron oxide (USPIO)-enhanced dynamic MRI studies were performed on rats. USPIO-enhanced MRI showed hypointensity on T_2*-weighted images in AR. However, the USPIO-particles are not only trapped in macrophages that accumulate in the allograft but also, as a downside, in other tissues or sites of infection or ischemia. In addition, the time interval between the application of the contrast agent and MRI assessment is quite long [5].

As a technique with possible approach for potential clinical translation of the MRI-based tracking of non-phagocytic cells, such as T- and B-lymphocytes, Liu et al. reported a new synthesized class of MRI contrast agent, IOPC-NH_2 particles (*Iron-oxide particles)*, to label T-cells in a rat model of the heart-lung transplant rejection [46]. Yet, it has not found its way into clinics because one major limitation of tracking labeled cells is that it is difficult to distinguish between live and dead labeled cells [47].

Other cellular and molecular MRI methods are based on the chemical exchange saturation transfer (CEST) MRI, which is sensitive in detecting molecules and metabolites without using a radio-isotope. Using glucose as a natural contrast agent and analyzing proton exchanges between the hydroxyl groups of glucose and water, this technique can be used to visualize metabolic changes in tissues and was first described in a study analyzing glucose uptake in tumors. The authors named this technique glucoCEST [48]. Recently, we demonstrated that glucoCEST is a feasible approach to diagnose AR in an allogenic rat renal transplant model [49]. GlucoCEST MRI was able to detect AR with high sensitivity (100%) and acceptable specificity (69%) (**Figure 3**). This tool was not only able to diagnose AR but also to detect treatment response early during rejection therapy; this could lead to a rapid adjust-

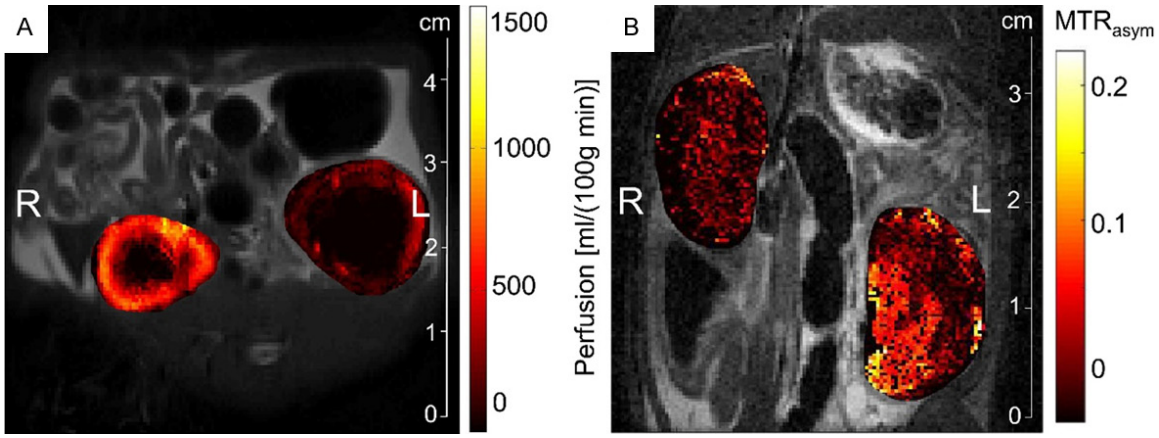

Figure 3. In vivo ASL (A) and glucoCEST (B) MRI showing representative ASL and glucoCEST MTR_{asym} maps of an allogeneically transplanted rat on day four post surgery. Decreased perfusion and increased glucose accumulation is detected especially in the cortex of the allograft on the right side (L) compared to the healthy right contralateral kidney on the left side (R).

ment of the therapeutic regimen. As this promising technique could have a relevant clinical impact on the management of kidney-transplanted patients, a patients study needs to be undertaken [49]. In addition to the techniques described above, several other MR-based methods have been recently described for renal allograft imaging, but not all of them focus currently on AR.

Magnetic resonance elastography (MRE), at this time, is not thought to be feasible to detect renal allograft rejection. Studies of elastography techniques (ultrasonic elastography, MRI) have been published, discussing the use of elastographic methods to detect organ stiffness in the progress of organ fibrosis rather than the processes of acute rejection of solid organ transplants [23, 50, 51].

Hemodynamic response imaging (HRI), another experimental approach to assess regional vascular reactivity, e.g. renovascular impairment due to hemodynamic chances, has not been discussed in the field of kidney transplantation yet. Milman et al. presented this technique in 2013. It is a BOLD MRI method, based on differences in the signal intensity in T_2*-weighted images generated in the course of the brief exposure to hypercapnia and hypercapnic-hyperoxia [23, 52]. As hemodynamic changes occur in acute allograft rejection, this method might be another diagnostic tool, but further studies in this research question are needed.

Computed tomography

Computed tomography (CT) is commonly available and generates X-ray-based images with high spatial resolution of the body. A CT can assess renal perfusion but needs the administration of an intravenous contrast agent. Given this, it may be helpful to detect AR and differentiate from ATN. However, as CT-based techniques rely on radiation and IV-contrast agents themselves can cause harm, CT has not yet been established in the clinical management of AR of renal allografts [5].

Conventional nuclear imaging

Conventional nuclear imaging methods are regularly applied to detect AR based on functional rather than morphological information. The gamma radiation from the deployed radioisotopes is directly measured by a crystal-based camera system planar or, when rotated around the body, by single photon emission computed tomography (SPECT). Commonly used isotopes in conventional nuclear imaging are ^{111}In, ^{67}Ga, ^{123}I and mainly ^{99m}Tc, the latter offering a wide application spectrum because of its relatively simple production, availability, and optimal decay characteristics [53]. Advantages of nuclear imaging include operator independency, high intrinsic sensitivity and availability of non-nephrotoxic tracers [5].

The broad application range in numerous diseases has continuously expanded during the

last years and pre-existing techniques have been optimized. Processes like tissue injury, bacterial infections, inflammation, and cell death (and other processes) can be detected and monitored using nuclear imaging techniques [29]. Due to the various pathophysiological processes related to renal AR, different markers for nuclear imaging have been developed during the last decades [29].

Already in 1976, George et al. visualized kidney AR using ^{99m}Tc-sulfur colloid, which accumulates in areas of fibrin thrombi in acute and chronic rejecting allografts [54]. At present, tracers used in either static scintigraphic imaging in AR detection or dynamic renal scintigraphy are suggested to have similar specificity. Of them, some authors propose, ^{99m}Tc-sulfur colloid might be the only one useful within a reasonable radiation dose. Unfortunately, computer-assisted analysis to compare tracer uptake in the region of interest with the uptake in the surrounding tissue showed a low sensitivity for ^{99m}Tc-sulfur colloid. Although this tracer is independent from the renal function, it does not accumulate in kidney allografts of patients receiving high-dose heparine or in kidneys with AR-associated necrosis. In conclusion, ^{99m}Tc-sulfur colloid-based imaging may not find its way into clinical routine [5].

In the case of allograft rejection, leukocyte recruitment plays an important role, and attempts have been made to label different immune cell lines *ex vivo* and *in vivo*. Common markers used for the radiolabeling of white blood cells in SPECT are ^{99m}TC-HMPAO or ^{111}In-oxine [55-57]. Compared to ^{18}F-FDG, these markers possess a higher compound stability and a longer half-life [58]. An important aspect in the usability of markers is the labeling efficiency, labeling stability, and viability of the labeled cells [5]. The accumulation of labeled cells can be affected by the background activity in the region of interest [59]. In kidney transplantation, a successful approach using ^{99m}Tc-HMPAO-labeled mononuclear cells was published showing the detection of rejection and discrimination from ATN with this approach [60].

For *in vivo* imaging, different ^{99m}Tc-, ^{111}In-, or ^{123}I-labeled antibodies have been developed to bind to CD3, CD4, CD25, or CD20 on immune cells [61]. Detection of AR in renal allografts was successfully shown for ^{99m}Tc-OKT3, a mouse monoclonal antibody against the CD3 complex on T cells [62]. The development of a humanized variant, namely the CD3 antibody ^{99m}Tc-SHNH-visilizumab, led to a significant reduction of the side effects by reduction of its immunogenicity [63, 64]. Since antibodies do not cross the endothelial barrier, such methods are limited to detect the intra- or peri-vascular antigens [5, 65].

Another approach to detect leukocyte accumulation in inflammation is to use a high-affinity radiolabeled ligand that binds to FPR1, a leukocyte receptor involved in chemotaxis and inflammatory responses of leukocytes. FPR1 expression is significantly upregulated during inflammation and the ^{99m}Tc-labeled FPR1 antagonist cFLFLFK-NH_2 has been shown to bind to FPR1 without effecting the physiology and functional response of the cells in the inflammatory processes [66].

A reporter gene-mediated method of radiolabeling regulatory T cells with ^{99m}Tc ($^{99m}TcO_4^-$) *in vitro* and *in vivo*, thereby enabling the precise visualization of the cells for as long as they are alive was presented by Sharif-Paghaleh et al. This labeling approach might become a useful tool in the setting of transplantation as well [67].

Complement activation is another important mechanism in inflammatory conditions besides the accumulation of immune cells. Recently, Sharif-Paghaleh et al. demonstrated a non-invasive imaging of complement activation in ischemia-reperfusion injury (IRI) in a murine cardiac transplantation model using the ^{99m}Tc-recombinant complement receptor 2 (^{99m}Tc-rCR2). As IRI and complement activation *per se* are involved in transplant rejection and complement inhibitors have been developed as a therapeutic agent, this technique may be a promising tool to identify tissue damage after transplantation, allow patient risk stratification, and monitor therapeutic interventions [68]. However, clinical studies are still missing.

Further, nuclear imaging can be routinely used for the monitoring of allograft function. While static imaging using ^{99m}Tc-dimercaptosuccinic acid (DMSA) can visualize functional kidney tissue and anatomical abnormalities, dynamic imaging using ^{99m}Tc-diethylenetriaminepentaacetic (DTPA) or ^{99m}Tc-mercaptoacetyltriglycine

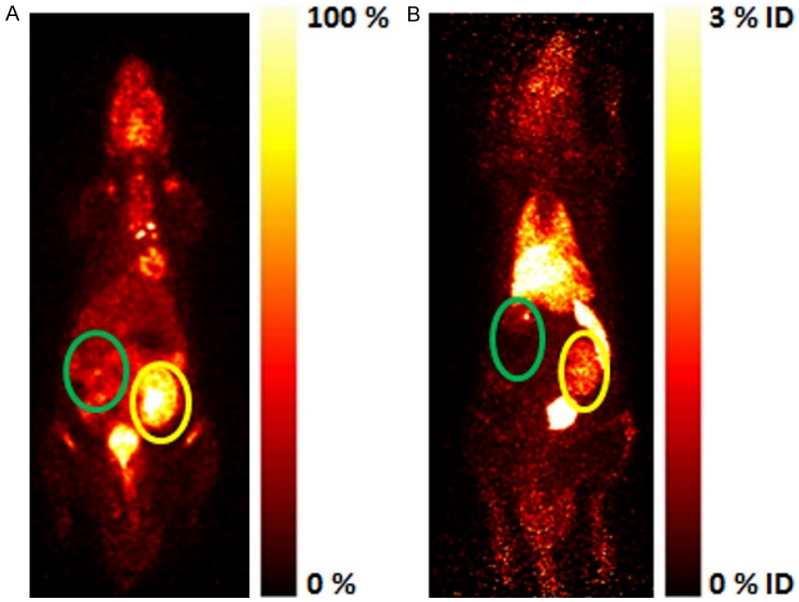

Figure 4. Representative PET-images of dynamic whole-body acquisitions of a allogeneically transplanted rat (postoperative day four, (A) after tail vein injection of 30 MBq ^{18}F-FDG (maximum a posterior projection, 180 min p.i.) and (B) after tail vein injection of 30·106 ^{18}F-FDG-labeled T cells (maximum-intensity projection, 50-70 min p.i.). While the allografts undergoing rejection show distinct enhancement of ^{18}F-FDG (yellow circles) the native control kidneys without rejection do not (green circles).

(MAG3) additionally allows the detection of AR and discrimination from ATN [69-74]. However, given the functional information derived from these approaches specificity for AR is rather low.

Positron emission tomography

Positron emission tomography (PET) is an imaging procedure based on the detection of radiation emitted through the electron-positron annihilation when positron emitting radionuclides are applied [5]: Usually, a radioactive tracer is administered intravenously and PET then captures the emitted gamma rays by a ring-shaped detector system. The benefits of nuclear imaging are whole body visualization with a high intrinsic sensitivity. Further, PET even copes with targets in a very low concentration range but provides a high specificity at the same time [61, 75]. It is successfully used for the assessment of metabolic processes and cellular events, such as apoptosis, and enables clinicians to visualize inflammation, changes in pH, and infection sites by using different tracers [76].

In 1978, the ^{18}F-Fluordeoxyglucose (FDG), a radioactive labeled glucose analog with a ^{18}F-fluorid substitution in the glucose molecule, for the scintigraphic detection of glucose metabolism was described and became the predominant radionuclide used in PET studies [77]. After injection, ^{18}F-FDG enters the cell via a glucose transporter like GLUT1 (Glucose transporter 1) and is phosphorylated by hexokinase. Contrary to "normal" glucose, FDG thereafter cannot enter glycolysis and becomes intracellularly trapped. Its signal intensity correlates with the cell's metabolic activity. Its whole body biodistribution can be assessed by PET [78].

The detection of glucose-based radionuclides by PET is not disease-specific and always has to be evaluated in the clinical context: For instance, the uptake of ^{18}F-FDG depends on the presence of glucose transporters and hexokinase activity, which underlie an upregulation under certain conditions, such as inflammation and tumor proliferation. Thus, the indications for the application of PET have grown over the last years: I.e. diseases such as vasculitis, fever of unknown origin, asthma, cystic fibrosis, and organ transplantation can be assessed [29].

We have established a non-invasive assessment of renal function by ^{18}F-fluoride clearance and shown that ^{18}F-FDG PET successfully detects AR in a rat renal transplant model [79, 80]. In the allograft setting, PET may be further used for the assessment of metabolic activity of recruited leucocytes, of renal function, of organic hypoxia, and of cell death. An ^{18}F-FDG-uptake during AR indicates a highly active metabolism in the graft, which is caused by the invading inflammatory cells (**Figure 4**).

The finding can be used to discriminate AR from other pathological conditions like ATN or drug toxicity [81]. Despite these specific signals in the renal transplant undergoing AR, the renal clearance of ^{18}F-FDG has to be taken into account. To avoid false positive ^{18}F-FDG signals in the kidney, we suggest the extension of time

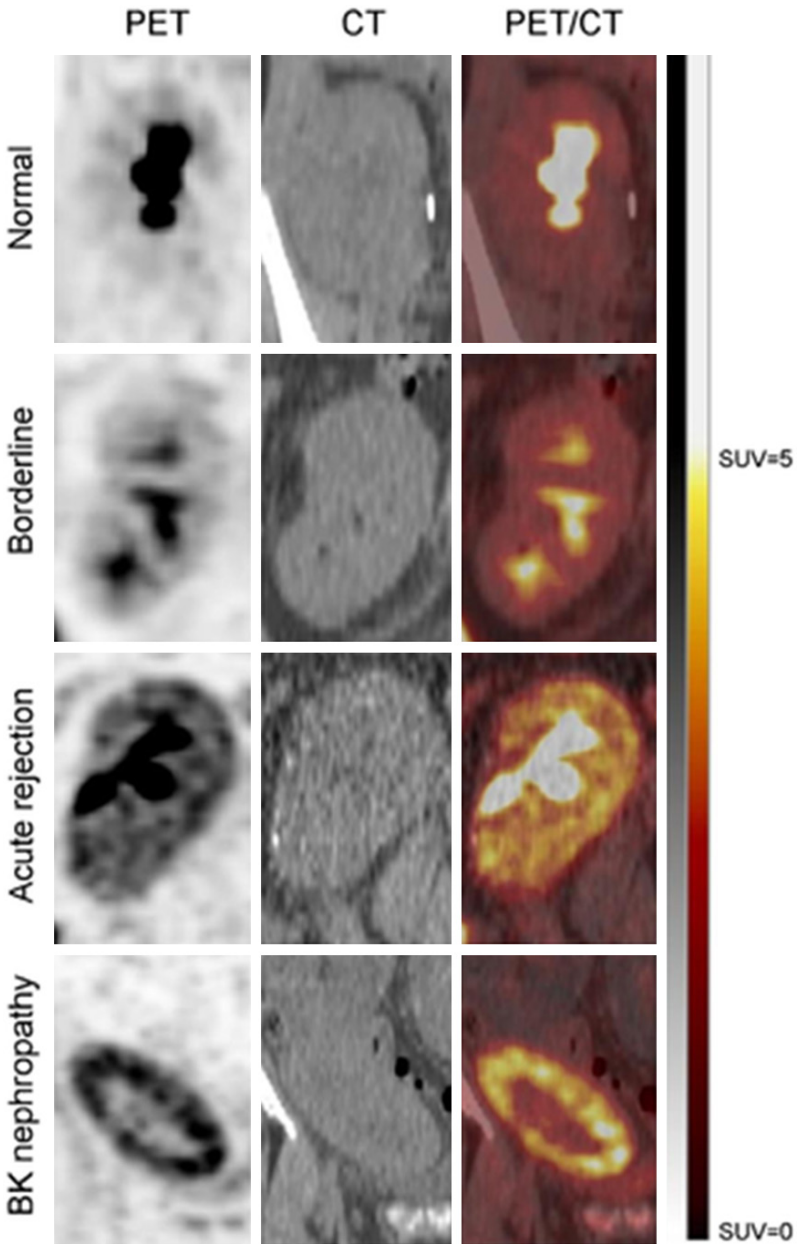

Figure 5. Representative ^{18}F-FDG PET/CT imaging in kidney transplant recipients with suspected acute rejection. PET (left column), CT (middle column), and combined PET/CT images taken after administration of ^{18}F-FDG are shown for kidney transplant recipients with biopsies showing normal histology, borderline changes, acute rejection or polyomavirus BK nephropathy. The arbitrary scale of SUVs (from 0 to 5) is illustrated on the right side. ^{18}F-FDG, fluorodeoxyglucose F18; CT, computed tomography; PET, positron emission tomography; SUV, standard uptake value. This image has been reprinted with permission from the paper [83].

between the application of the tracer and the PET measurement or to use ^{18}F-FDG labelled T-cells [81, 82]. However, producing ^{18}F-FDG labelled T-cells in humans might be time consuming and effortful [5]. Interestingly, the ^{18}F-FDG uptake of renal allografts immediately disappears after the successful treatment of AR suggesting a potential of ^{18}F-FDG PET for serial monitoring of treatment efficacy [79]. Recently, Lovinfosse et al. combined PET and CT to analyze a cohort of kidney-transplanted patients with suspected AR. A positive correlation was found between the tracer-uptake in the allograft and the histologic degree of rejection (**Figure 5**). This method had a 100% sensitivity but only a 50% specificity; the authors postulated that this low specificity in detecting AR may be due to the nature of ^{18}F-FDG [5, 83].

Conclusions

Non-invasive methods for a specific diagnosis of AR and the monitoring of the allograft function are of great interest. Advances in technology and tracer development have opened up new possibilities in this regard. Especially, novel combinations of different methods and techniques may overcome the inherent limitations of individual techniques for the non-invasive diagnosis of AR. Although promising, at present most of these new technologies are still at an experimental stage, have limitations e.g., in differentiation of acute antibody-mediated and cellular rejection, making them very useful research tools but not yet ready for routine clinical applications.

Acknowledgements

We acknowledge support by The Collaborative Research Centre 656 (Deutsche Forschungsgemeinschaft, SFB656, Projects C7 and PM12 and 21). The funders had no role in study desi-

gn, data collection and analysis, decision to publish, or preparation of the manuscript.

Disclosure of conflict of interest

None.

Abbreviations

ADC, Apparent Diffusion Coefficient; AFRI, Acoustic Radiation Force Impulse Imaging; AMR, Acute antibody-mediated rejection; AR, Acute rejection; ASL, Arterial spin labeling; ATN, Acute tubular necrosis; BOLD, Blood-oxygen level-dependent; CD, Cluster of Differentiation; CEST, Chemical exchange saturation transfer; CEUS, Contrast-enhanced ultrasound; cFLFLFK-NH_{2-c}, innamoyl-phenylalanine-(D) leucine-phenylalanine-(D) leucine-phenylalanine lysine - amidogen; CPP, Cortex-pelvis proportion; CSA, Cyclosporine A; CT, Computed tomography; DCE, Dynamic Contrast Enhanced; DMSA, ^{99m}Tc-dimercaptosuccinic acid; DTI, Diffusion tensor imaging; DTPA, ^{99m}Tc-diethylenetriaminepentaacetic acid; DWI, Diffusion-weighted; FDG, F-Fluordeoxyglucose; FPR1, Formyl peptide receptor 1; IRI, Ischemia-reperfusion injury; KTx, Kidney transplantation; MAG3, ^{99m}Tc-mercaptoacetyltriglycine; MR, Magnetic resonance; MRI, Magnetic resonance imaging; MRNU, MR Nephro-Urography; PET, Positron emission tomography; PI, Pulsatility index; RI, Resistive index; SDI, Serial duplex index; SPECT, Single photon emission computed tomography; SWEI, Shear-wave-sonoelastography; USPIO, Ultrasmall supermagnetic iron oxide; ^{111}In, Indium-111; ^{123}I, Iodine-123; ^{67}Ga, Gallium-67; ^{99m}Tc, Technetium-99m; ^{99m}TC-HMPAO, Technetium-99m exametazime (hexamethylpropyleneamine oxime); ^{99m}Tc-O_4^-, Technetium-99m pertechnetate; ^{99m}Tc-O-KT3, Technetium-99m Muromonab-CD3; ^{99m}Tc-rCR2, Technetium-99m recombinant complement receptor 2; ^{99m}Tc-SHNH-visilizumab, Technetium-99m succinimidyl-6-hydrazinonicotinate hydrochloride-conjugated visilizumab; VISR, Viscoelastic response ultrasound.

Address correspondence to: Stefan Reuter, Department of Medicine, Division of General Internal Medicine, Nephrology and Rheumatology, University Hospital of Muenster, 48149 Muenster, Germany. Tel: +49-251-83-47540; Fax: +49-251-83-45813; E-mail: sreuter@uni-muenster.de

References

[1] Wolfe RA, Ashby VB, Milford EL, Ojo AO, Ettenger RE, Agodoa LY, Held PJ and Port FK. Comparison of mortality in all patients on dialysis, patients on dialysis awaiting transplantation and recipients of a first cadaveric transplant. N Engl J Med 1999; 341: 1725-1730.

[2] Tabriziani H, Lipkowitz MS and Vuong N. Chronic kidney disease, kidney transplantation and oxidative stress: a new look to successful kidney transplantation. Clin Kidney J 2017; 11: 130-135.

[3] Elbadri A, Traynor C, Veitch JT, O'Kelly P, Magee C, Denton M, O'Sheaghdha C and Conlon PJ. Factors affecting eGFR 5-year post-deceased donor renal transplant: analysis and predictive model. Ren Fail 2015; 37: 417-423.

[4] Jalalzadeh M, Mousavinasab N, Peyrovi S and Ghadiani MH. The impact of acute rejection in kidney transplantation on long-term allograft and patient outcome. Nephrourol Mon 2015; 7: e24439.

[5] Hanssen O, Erpicum P, Lovinfosse P, Meunier P, Weekers L, Tshibanda L, Krzesinski JM, Hustinx R and Jouret F. Non-invasive approaches in the diagnosis of acute rejection in kidney transplant recipients. Part I. in vivo imaging methods. Clin Kidney J 2017; 10: 97-105.

[6] Tsai SF, Chen CH, Shu KH, Cheng CH, Yu TM, Chuang YW, Huang ST, Tsai JL and Wu MJ. Current safety of renal allograft biopsy with indication in adult recipients. Med 2016; 95: 1-7.

[7] Meier M, Fricke L, Eikenbusch K, Smith E, Kramer J, Lehnert H and Nitschke M. The serial duplex index improves differential diagnosis of acute renal transplant dysfunction. J Ultrasound Med 2017; 36: 1607-1615.

[8] Viazzi F, Leoncini G, Derchi LE and Pontremoli R. Ultrasound Doppler renal resistive index: a useful tool for the management of the hypertensive patient. J Hypertens 2014; 32: 149-153.

[9] Naesens M, Heylen L, Lerut E, Claes K, De Wever L, Claus F, Oyen R, Kuypers D, Evenepoel P, Bammens B, Sprangers B, Meijers B, Pirenne J, Monbaliu D, de Jonge H, Metalidis C, De Vusser K and Vanrenterghem Y. Intrarenal resistive index after renal transplantation. N Engl J Med 2013; 369: 1797-1806.

[10] Radermacher J, Mengel M, Ellis S, Stuht S, Hiss M, Schwarz A, Eisenberger U, Burg M, Luft FC, Gwinner W and Haller H. The renal arterial resistance index and renal allograft survival. N Engl J Med 2003; 349: 115-124.

[11] Kramann R, Frank D, Brandenburg VM, Heussen N, Takahama J, Krüger T, Riehl J and Floege J. Prognostic impact of renal arterial resistance index upon renal allograft survival: the time point matters. Nephrol Dial Transplant 2012; 27: 3958-3963.

[12] Perrella RR, Duerinckx AJ, Tessler FN, Danovitch GM, Wilkinson A, Gonzalez S, Cohen AH and Grant EG. Evaluation of renal transplant

dysfunction by duplex Doppler sonography: a prospective study and review of the literature. Am J Kidney Dis 1990; 15: 544-550.
[13] Shebel HM, Akl A, Dawood A, El-Diasty TA, Shokeir AA and Ghoneim MA. Power doppler sonography in early renal transplantation: does it differentiate acute graft rejection from acute tubular necrosis? Saudi J Kidney Dis Transpl 2014; 25: 733-740.
[14] Ghonge NP, Mohan M, Kashyap V and Jasuja S. Renal allograft dysfunction: evaluation with shear-wave sonoelastography. Radiology 2018; 288: 146-152.
[15] Stock KF, Klein BS, Cong MT, Regenbogen C, Kemmner S, Büttner M, Wagenpfeil S, Matevossian E, Renders L, Heemann U and Küchle C. ARFI-based tissue elasticity quantification and kidney graft dysfunction: first clinical experiences. Clin Hemorheol Microcirc 2011; 49: 527-535.
[16] Yang C, Hu M, Zhu T and He W. Evaluation of kidney allograft status using novel ultrasonic technologies. Asian J Urol 2015; 2: 142-150.
[17] Hossain MM, Selzo MR, Hinson RM, Baggesen LM, Detwiler RK, Chong WK, Burke LM, Caughey MC, Fisher MW, Whitehead SB and Gallippi CM. Evaluating renal transplant status using viscoelastic response (visr) ultrasound. Ultrasound Med Biol 2018; 44: 1573-1584.
[18] Mueller-Peltzer K, Negrão de Figueiredo G, Fischereder M, Habicht A, Rübenthaler J and Clevert DA. Vascular rejection in renal transplant: Diagnostic value of contrast-enhanced ultrasound (CEUS) compared to biopsy. Clin Hemorheol Microcirc 2018; 69: 77-82.
[19] Grabner A, Kentrup D, Mühlmeister M, Pawelski H, Biermann C, Bettinger T, Pavenstädt H, Schlatter E, Tiemann K and Reuter S. Noninvasive imaging of acute renal allograft rejection by ultrasound detection of microbubbles targeted to t-lymphocytes in rats. Ultraschall Med 2015; 37: 82-91.
[20] Grabner A, Kentrup D, Pawelski H, Mühlmeister M, Biermann C, Edemir B, Heitplatz B, Van Marck V, Bettinger T, Pavenstädt H, Schlatter E, Stypmann J, Tiemann K and Reuter S. Renal contrast-enhanced sonography findings in a model of acute cellular allograft rejection. Am J Transplant 2016; 16: 1612-1619.
[21] Liao T, Zhang Y, Ren J, Zheng H, Zhang H, Li X, Liu X, Yin T and Sun Q. Noninvasive quantification of intrarenal allograft C4d deposition with targeted ultrasound imaging. Am J Transplant 2019; 19: 259-268.
[22] Zhang JL, Morrell G, Rusinek H, Sigmund EE, Chandarana H, Lerman LO, Prasad PV, Niles D, Artz N, Fain S, Vivier PH, Cheung AK and Lee VS. New magnetic resonance imaging methods in nephrology. Kidney Int 2014; 85: 768-778.
[23] van Eijs MJM, van Zuilen AD, de Boer A, Froeling M, Nguyen TQ, Joles JA, Leiner T and Verhaar MC. Innovative perspective: gadolinium-free magnetic resonance imaging in long-term follow-up after kidney transplantation. Front Physiol 2017; 8: 1-12.
[24] Huang Y, Sadowski EA, Artz NS, Seo S, Djamali A, Grist TM and Fain SB. Measurement and comparison of T1 relaxation times in native and transplanted kidney cortex and medulla. J Magn Reson Imaging 2011; 33: 1241-1247.
[25] Abou-El-Ghar ME, El-Diasty TA, El-Assmy AM, Refaie HF, Refaie AF and Ghoneim MA. Role of diffusion-weighted MRI in diagnosis of acute renal allograft dysfunction: a prospective preliminary study. Br J Radiol 2012; 85: e206-211.
[26] Caroli A, Schneider M, Friedli I, Ljimani A, De Seigneux S, Boor P, Gullapudi L, Kazmi I, Mendichovszky IA, Notohamiprodjo M, Selby NM, Thoeny HC, Grenier N and Vallée JP. Diffusion-weighted magnetic resonance imaging to assess diffuse renal pathology: a systematic review and statement paper. Nephrol Dial Transplant 2018; 33: ii29-40.
[27] Hueper K, Gutberlet M, Bräsen JH, Jang MS, Thorenz A, Chen R, Hertel B, Barrmeyer A, Schmidbauer M, Meier M, Von Vietinghoff S, Khalifa A, Hartung D, Haller H, Wacker F, Rong S and Gueler F. Multiparametric functional MRI: non-invasive imaging of inflammation and edema formation after kidney transplantation in mice. PLoS One 2016; 11: 1-15.
[28] Deger E, Celik A, Dheir H, Turunc V, Yardimci A, Torun M and Cihangiroglu M. Rejection evaluation after renal transplantation using MR diffusion tensor imaging. Acta radiol 2018; 59: 876-883.
[29] Thölking G, Schuette-Nuetgen K, Kentrup D, Pawelski H and Reuter S. Imaging-based diagnosis of acute renal allograft rejection. World J Transplant 2016; 6: 174.
[30] Lanzman RS, Ljimani A, Pentang G, Zgoura P, Zenginli H, Kröpil P, Heusch P, Schek J, Miese FR, Blondin D, Antoch G and Wittsack HJ. Kidney transplant: functional assessment with diffusion-tensor MR imaging at 3T. Radiology 2013; 266: 218-225.
[31] Liu G, Han F, Xiao W, Wang Q, Xu Y and Chen J. Detection of renal allograft rejection using blood oxygen level-dependent and diffusion weighted magnetic resonance imaging: a retrospective study. BMC Nephrol 2014; 15: 158.
[32] Sadowski EA, Djamali A, Wentland AL, Muehrer R, Becker BN, Grist TM and Fain SB. Blood oxygen level-dependent and perfusion magnetic resonance imaging: detecting differences in oxygen bioavailability and blood flow in transplanted kidneys. Magn Reson Imaging 2010; 28: 56-64.

[33] Taffel MT, Nikolaidis P, Beland MD, Blaufox MD, Dogra VS, Goldfarb S, Gore JL, Harvin HJ, Heilbrun ME, Heller MT, Khatri G, Preminger GM, Purysko AS, Smith AD, Wang ZJ, Weinfeld RM, Wong-You-Cheong JJ, Remer EM and Lockhart ME. ACR Appropriateness Criteria® Renal Transplant Dysfunction. J Am Coll Radiol 2017; 14: S272-281.

[34] Yan Y, Sun X and Shen B. Contrast agents in dynamic contrast-enhanced magnetic resonance imaging. Oncotarget 2017; 8: 43491-43505.

[35] Kalb B, Martin DR, Salman K, Sharma P, Votaw J and Larsen C. Kidney transplantation: structural and functional evaluation using MR Nephro-Urography. J Magn Reson Imaging 2008; 28: 805–822.

[36] Wentland AL, Sadowski EA, Djamali A, Grist TM, Becker BN and Fain SB. Quantitative MR measures of intrarenal perfusion in the assessment of transplanted kidneys. Acad Radiol 2009; 16: 1077-1085.

[37] Khalifa F, Abou El-Ghar M, Abdollahi B, Frieboes HB, El-Diasty T and El-Baz A. A comprehensive non-invasive framework for automated evaluation of acute renal transplant rejection using DCE-MRI. NMR Biomed 2013; 26: 1460-1470.

[38] Daftari Besheli L, Aran S, Shaqdan K, Kay J and Abujudeh H. Current status of nephrogenic systemic fibrosis. Clin Radiol 2014; 69: 661-668.

[39] Ranga A, Agarwal Y and Garg K. Gadolinium based contrast agents in current practice: risks of accumulation and toxicity in patients with normal renal function. Indian J Radiol Imaging 2017; 27: 141.

[40] Gadolinium-haltige kontrastmittel: aktualisierte empfehlungen nach bewertung von gadoliniumablagerungen im gehirn und anderen geweben. 2018. URL: https://www.akdae.de/Arzneimittelsicherheit/RHB/Archiv/2018/20-180108.pdf.

[41] Hueper K, Schmidbauer M, Thorenz A, Bräsen JH, Gutberlet M, Mengel M, Hartung D, Chen R, Meier M, Haller H, Wacker F, Rong S and Gueler F. Longitudinal evaluation of perfusion changes in acute and chronic renal allograft rejection using arterial spin labeling in translational mouse models. J Magn Reson Imaging 2017; 46: 1664-1672.

[42] Lanzman RS, Wittsack HJ, Martirosian P, Zgoura P, Bilk P, Kröpil P, Schick F, Voiculescu A and Blondin D. Quantification of renal allograft perfusion using arterial spin labeling MRI: initial results. Eur Radiol 2010; 20: 1485-1491.

[43] Thurman JM and Serkova NJ. Nanosized contrast agents to noninvasively detect kidney inflammation by magnetic resonance imaging. Adv Chronic Kidney Dis 2013; 20: 488-499.

[44] Hauger O, Grenier N, Deminère C, Lasseur C, Delmas Y, Merville P and Combe C. USPIO-enhanced MR imaging of macrophage infiltration in native and transplanted kidneys: initial results in humans. Eur Radiol 2007; 17: 2898-2907.

[45] Chae EY, Song EJ, Sohn JY, Kim ST, Woo CW, Gong G, Kang HJ and Lee JS. Allogeneic renal graft rejection in a rat model: in vivo MR imaging of the homing trait of macrophages. Radiology 2010; 256: 847-854.

[46] Liu L, Ye Q, Wu Y, Hsieh WY, Chen CL, Shen HH, Wang SJ, Zhang H, Hitchens TK and Ho C. Tracking T-cells in vivo with a new nano-sized MRI contrast agent. Nanomedicine 2012; 8: 1345-1354.

[47] Ngen E and Artemov D. Advances in monitoring cell-based therapies with magnetic resonance imaging: future perspectives. Int J Mol Sci 2017; 18: 198.

[48] Walker-Samuel S, Ramasawmy R, Torrealdea F, Rega M, Rajkumar V, Johnson SP, Richardson S, Gonçalves M, Parkes HG, Årstad E, Thomas DL, Pedley RB, Lythgoe MF and Golay X. In vivo imaging of glucose uptake and metabolism in tumors. Nat Med 2013; 19: 1067-1072.

[49] Kentrup D, Bovenkamp P, Busch A, Schuette-Nuetgen K, Pawelski H, Pavenstädt H, Schlatter E, Herrmann KH, Reichenbach JR, Löffler B, Heitplatz B, Van Marck V, Yadav NN, Liu G, van Zijl PCM, Reuter S and Hoerr V. GlucoCEST magnetic resonance imaging in vivo may be diagnostic of acute renal allograft rejection. Kidney Int 2017; 92: 757-764.

[50] Sarvazyan A, Hall TJ, Urban MW, Fatemi M, Aglyamov SR and Garra BS. An overview of elastography - an emerging branch of medical imaging. Curr Med Imaging Rev 2011; 7: 255-282.

[51] Wang YT. Functional assessment of transplanted kidneys with magnetic resonance imaging. World J Radiol 2015; 7: 343.

[52] Milman Z, Heyman SN, Corchia N, Edrei Y, Axelrod JH, Rosenberger C, Tsarfati G and Abramovitch R. Hemodynamic response magnetic resonance imaging: application for renal hemodynamic characterization. Nephrol Dial Transplant 2013; 28: 1150-1156.

[53] Pimlott SL and Sutherland A. Molecular tracers for the PET and SPECT imaging of disease. Chem Soc Rev 2011; 40: 149-162.

[54] George EA, Codd JE, Newton WT, Haibach H and Donati RM. Comparative evaluation of renal transplant rejection with radioiodinated fibrinogen ^{99m}Tc-sulfur collid, and ^{67}Ga-citrate. J Nucl Med 1976; 17: 175-180.

[55] Datz FL. Indium-111-labeled leukocytes for the detection of infection: current status. Semin Nucl Med 1994; 24: 92-109.

[56] Peters AM, Danpure HJ, Osman S, Hawker RJ, Henderson BL, Hodgson HJ, Kelly JD, Neirinckx RD and Lavender JP. Clinical experience with ^{99m}Tc-hexamethylpropylene-amineoxime for labelling leucocytes and imaging inflammation. Lancet 1986; 2: 946-949.

[57] McAfee JG and Thakur ML. Survey of radioactive agents for in vitro labeling of phagocytic leukocytes. I. Soluble agents. J Nucl Med 1976; 17: 480-487.

[58] Forstrom LA, Dunn WL, Mullan BP, Hung JC, Lowe VJ and Thorson LM. Biodistribution and dosimetry of [(18)F]fluorodeoxyglucose labelled leukocytes in normal human subjects. Nucl Med Commun 2002; 23: 721-725.

[59] Sanches A, Etchebehere ECSC, Mazzali M, Filho GA, Lima MCL, Santos AO, Ramos CD, Cardinalli I, Billis A and Camargo EE. The accuracy of (99m)Tc-DTPA scintigraphy in the evaluation of acute renal graft complications. Int Braz J Urol 2003; 29: 507-516.

[60] Lopes de Souza SA, Barbosa da Fonseca LM, Torres Gonçalves R, Salomão Pontes D, Holzer TJ, Proença Martins FP and Gutfilen B. Diagnosis of renal allograft rejection and acute tubular necrosis by ^{99m}Tc-mononuclear leukocyte imaging. Transplant Proc 2004; 36: 2997-3001.

[61] Signore A, Mather SJ, Piaggio G, Malviya G and Dierckx RA. Molecular imaging of inflammation/infection: nuclear medicine and optical imaging agents and methods. Chem Rev 2010; 110: 3112-3145.

[62] Martins FP, Souza SA, Gonçalves RT, Fonseca LM and Gutfilen B. Preliminary results of [^{99m}Tc]OKT3 scintigraphy to evaluate acute rejection in renal transplants. Transplant Proc 2004; 36: 2664-2667.

[63] Cole MS, Stellrecht KE, Shi JD, Homola M, Hsu DH, Anasetti C, Vasquez M and Tso JY. HuM-291, a humanized anti-CD3 antibody, is immunosuppressive to T cells while exhibiting reduced mitogenicity in vitro. Transplantation 1999; 68: 563-571.

[64] Shan L. ^{99m}Tc-Labeled succinimidyl-6-hydrazinonicotinate hydrochloride (SHNH)-conjugated visilizumab. Molecular Imaging and Contrast Agent Database (MICAD). 2010. URL: https://www.ncbi.nlm.nih.gov/books/NBK23621/.

[65] Pawelski H, Schnöckel U, Kentrup D, Grabner A, Schäfers M and Reuter S. SPECT- and PET-based approaches for noninvasive diagnosis of acute renal allograft rejection. Biomed Res Int 2014; 2014: 1-7.

[66] Stasiuk GJ, Holloway PM, Rivas C, Trigg W, Luthra SK, Morisson Iveson V, Gavins FN and Long NJ. ^{99m}Tc SPECT imaging agent based on cFLFLFK for the detection of FPR1 in inflammation. Dalt Trans 2015; 44: 4986-4993.

[67] Sharif-Paghaleh E, Sunassee K, Tavaré R, Ratnasothy K, Koers A, Ali N, Alhabbab R, Blower PJ, Lechler RI, Smyth LA, Mullen GE and Lombardi G. In vivo SPECT reporter gene imaging of regulatory T cells. PLoS One 2011; 6: e25857.

[68] Sharif-Paghaleh E, Yap ML, Meader LL, Chuamsaamarkkee K, Kampmeier F, Badar A, Smith RA, Sacks S and Mullen GE. Noninvasive imaging of activated complement in ischemia-reperfusion injury post-cardiac transplant. Am J Transplant 2015; 15: 2483-2490.

[69] Budihna NV, Milcinski M, Kajtna-Koselj M and Malovrh M. Relevance of Tc-99m DMSA scintigraphy in renal transplant parenchymal imaging. Clin Nucl Med 1994; 19: 782-784.

[70] Even-Sapir E, Gutman M, Lerman H, Kaplan E, Ravid A, Livshitz G and Nakache R. Kidney allografts and remaining contralateral donor kidneys before and after transplantation: assessment by quantitative (99m)Tc-DMSA SPECT. J Nucl Med 2002; 43: 584-588.

[71] Dubovsky EV, Russell CD, Bischof-Delaloye A, Bubeck B, Chaiwatanarat T, Hilson AJ, Rutland M, Oei HY, Sfakianakis GN and Taylor A. Report of the radionuclides in nephrourology committee for evaluation of transplanted kidney (review of techniques). Semin Nucl Med 1999; 29: 175-188.

[72] Sfakianaki E, Sfakianakis GN, Georgiou M and Hsiao B. Renal scintigraphy in the acute care setting. Semin Nucl Med 2013; 43: 114-128.

[73] Sfakianakis GN, Sfakianaki E, Georgiou M, Serafini A, Ezuddin S, Kuker R, Zilleruelo G, Strauss J, Abitbol C, Chandar J, Seeherunvong W, Bourgoignie J, Roth D, Leveillee R, Bird VG, Block N, Gosalbez R, Labbie A, Guerra JJ and Yrizarry J. A Renal protocol for all ages and all indications: mercapto-Acetyl-triglycine (MAG3) with simultaneous injection of furosemide (MAG3-F0): a 17-year experience. Semin Nucl Med 2009; 39: 156-173.

[74] Sundaraiya S, Mendichovszky I, Biassoni L, Sebire N, Trompeter RS and Gordon I. Tc-99m DTPA renography in children following renal transplantation - its value in the evaluation of rejection. Pediatr Transplant 2007; 11: 771-776.

[75] Hall LT, Struck AF and Perlman SB. Clinical molecular imaging with PET agents other than ^{18}F-FDG. Curr Pharm Biotechnol 2010; 11: 545-554.

[76] Skotland T. Molecular imaging: challenges of bringing imaging of intracellular targets into common clinical use. Contrast Media Mol Imaging 2012; 7: 1-6.

[77] Gallagher BM, Fowler JS, Gutterson NI, MacGregor RR, Wan CN and Wolf AP. Metabolic trapping as a principle of oradiopharmaceutical design: some factors resposible for the bio-

distribution of [^{18}F] 2-deoxy-2-fluoro-D-glucose. J Nucl Med 1978; 19: 1154-1161.

[78] Pauwels EK, Ribeiro MJ, Stoot JH, McCready VR, Bourguignon M and Mazière B. FDG accumulation and tumor biology. Nucl Med Biol 1998; 25: 317-322.

[79] Reuter S, Schnockel U, Edemir B, Schroter R, Kentrup D, Pavenstadt H, Schober O, Schlatter E, Gabriels G and Schafers M. Potential of Noninvasive serial assessment of acute renal allograft rejection by ^{18}F-FDG PET to monitor treatment efficiency. J Nucl Med 2010; 51: 1644-1652.

[80] Schnöckel U, Reuter S, Stegger L, Schlatter E, Schäfers KP, Hermann S, Schober O, Gabriëls G and Schäfers M. Dynamic ^{18}F-fluoride small animal PET to noninvasively assess renal function in rats. Eur J Nucl Med Mol Imaging 2008; 35: 2267-2274.

[81] Reuter S, Schnöckel U, Schröter R, Schober O, Pavenstädt H, Schäfers M, Gabriëls G and Schlatter E. Non-invasive imaging of acute renal allograft rejection in rats using small animal ^{18}F-FDG-PET. PLoS One 2009; 4: e5296.

[82] Grabner A, Kentrup D, Edemir B, Sirin Y, Pavenstadt H, Schlatter E, Schober O, Schafers M, Schnockel U and Reuter S. PET with ^{18}F-FDG-Labeled T lymphocytes for diagnosis of acute rat renal allograft rejection. J Nucl Med 2013; 54: 1147-1153.

[83] Lovinfosse P, Weekers L, Bonvoisin C, Bovy C, Grosch S, Krzesinski JM, Hustinx R and Jouret F. Fluorodeoxyglucose F^{18} positron emission tomography coupled with computed tomography in suspected acute renal allograft rejection. Am J Transplant 2016; 16: 310-316.